Materials Chemistry and Physics 138 (2013) 303–312

Contents lists available at SciVerse ScienceDirect

Materials Chemistry and Physics

journal homepage: www.elsevier.com/locate/matchemphys

Acrylonitrile-capped poly(propyleneimine) dendrimer curing agent for epoxy resins: Model-free isoconversional curing kinetics, thermal decomposition and mechanical properties

Jintao Wan [a,b], Cheng Li [a], Zhi-Yang Bu [a,*], Hong Fan [a,**], Bo-Geng Li [a]

[a] State Key Laboratory of Chemical Engineering, Department of Chemical and Biochemical Engineering, Zhejiang University, Hangzhou 310027, China
[b] Zhejiang Jiamin Plastics Co. Ltd., Jiaxing 314027, China

HIGHLIGHTS

- We compare the isoconversional curing kinetics of DGEBA/1.0GPPI and DGEBA/PAN4.
- Acrylonitrile-capped PAN4 is much lower reactive than controlled 1.0GPPI.
- TG analysis shows the two cured epoxy systems are thermally stable up to 200 °C.
- DMA results reveal the viscoelastic response of the two cured networks differs greatly.
- PAN4 greatly improves the shear, impact strengths and processability of the epoxy.

ARTICLE INFO

Article history:
Received 4 February 2012
Received in revised form
13 November 2012
Accepted 24 November 2012

Keywords:
Polymers
Differential scanning calorimetry (DSC)
Computer modelling and simulation
Thermogravimetric analysis (TGA)
Mechanical properties

ABSTRACT

Acrylonitrile-modified aliphatic amine adducts are often used as curing agents for room-temperature epoxy formulations (coatings, adhesives, sealants, castings, etc.), yet the curing reaction and properties of resultant epoxy systems still remain less fundamentally understood. Herein we systematically investigate our newly-developed acrylonitrile-modified multifunctional polyamine curing agent for bisphenol A epoxy resin (DGEBA): an acrylonitrile-capped poly(propyleneimine) dendrimer (PAN4). The impact of the molecular structure of PAN4 and a controlled poly(propyleneimine) dendrimer (1.0GPPI) on the curing reactivity, reaction mechanisms, thermal stability, viscoelastic response and mechanical properties of the epoxy systems are highlighted. Differential scanning calorimetry (DSC) confirms DGEBA/PAN4 shows markedly lower reactivity and reaction exotherm than DGEBA/1.0GPPI, and the model-free isoconversional kinetic analysis reveals that DGEBA/PAN4 has the generally lower reaction activation energy. To be quantitative, the progress of the isothermal cure is predicted from the dynamic cure by using the Vyazovkin equation. The isothermal kinetic prediction shows that DGEBA/PAN4 requires about 10 times longer time to achieve the same conversion than DGEBA/1.0GPPI, which agrees with the experimentally observed much longer gel time of DGEBA/PAN4. Subsequently, dynamic mechanical analysis shows that PAN4 results in the cured epoxy network with the lower β- and glass-relaxation temperatures, crosslink density, relaxation activation energy, enthalpy, entropy, but the higher damping near room temperature than 1.0GPPI. Finally, thermogravimetric analysis (TGA) demonstrates cured DGEBA/PAN4 is thermally stable up to 200 °C, and mechanical property tests substantiate that PAN4 endows the cured epoxy with much higher impact and adhesion strengths than 1.0GPPI. Our data can provide a deeper insight into acrylonitrile-modified aliphatic amine curing agents from the two good model compounds (PAN4 and 1.0GPPI).

1. Introduction

Epoxy resins have many attractive properties such as high adhesion strength, dimension stability, low cure shrinkage, excellent chemical and heat resistance, formulation diversity, favorable processability, etc., hence accounting for their extensive

* Corresponding author. Tel.: +86 571 87952631; fax: +86 571 87951612.
** Corresponding author. Tel.: +86 571 87957371; fax: +86 571 87951612.
E-mail addresses: wan_jintao@yahoo.com.cn (J. Wan), buzhiyang@zju.edu.cn (Z.-Y. Bu), hfan@zju.edu.cn (H. Fan).

0254-0584/$ – see front matter © 2012 Elsevier B.V. All rights reserved.
http://dx.doi.org/10.1016/j.matchemphys.2012.11.060

applications in anticorrosive coatings, composite matrices, potting materials, electronic-packaging molding compounds, structural adhesives, sealants, and so on [1–3]. Uncured epoxy resins are composed of monomers and/or oligomers having two or more reactive epoxy groups, and in practical applications they must be transformed to a highly crosslinked network in the presence of curing agents. The most wildly used epoxy resins holding about 80% market share belong to the bisphenol-A type with different molecular weight ranges. The ultimate bulk properties of epoxy resins depend strongly on properly selecting a properly selected curing agent under optimal curing conditions. In general, epoxy curing agents include amines, acid anhydride, phenolic resins, mercaptans, etc., among which amines are the most important. In particular, aliphatic amines are highly reactive and can cure epoxy resins well even at room temperature, so that they find vast usages in room-temperature epoxy coatings and adhesives.

Nevertheless, conventional aliphatic-amine curing agents have low molecular weights, which leads to their high volatility, strong toxicity, skin sensitization, very strict dosage, "surface flush" resulting from the rapid absorption of carbon dioxide and vapor in air, and so on [4,5]. For this reason, usually low-molecular-weight aliphatic amine curing agents are modified chemically to increase molecular weights and to achieve desired properties such as reduced volatility and toxicity, increased dosage and pot life, improved flexibility, surface appearance and mechanical performances, etc., and they are most frequently modified by acrylonitrile or butyl-glycidylether. On the other hand, recently the use of dendritic aliphatic amino-terminated dendrimers such as poly(-propyleneimine) (PPIs) [6–12], polyamidoamine (PAMAMs) [13,14] and poly(ester-amine) (PEAs) [15] as novel curing agents are capturing increasing research interest. These dendrimers have the much high molecular weights combined with extraordinarily high functionalities compared to conventional aliphatic amines, so that they show low volatility and high reactivity. More interestingly, PPIs, consisting only of C–C and C–N linkages, can be used as raw materials to produce novel amine adducts by a suitable chemical modification method [16,17]. These resulting amine adducts may have more sophisticated properties, because PPIs have the high functionalities, reactivity, branched molecular structure, and excellent thermal stability.

For example, in 2011 we reported two kinds of novel amine adduct curing agents for epoxy resins: butylglycidylether-modified poly(propyleneimine) dendrimers (PB2 and PB4) [16] and acrylonitrile-capped poly(propyleneimine) dendrimer (PAN4) [17]. We found that curing reaction of the epoxy systems are greatly affected by the attached butylglycidylether and acrylonitrile moieties of these curing agents. In particular, as demonstrated in Scheme 1, PAN4 has four reactive amino groups with high nitrile group content and precise molecular symmetry. We have established a rate equation to predict the nonisothermal curing rate constant of DGEBA/PAN4. Nevertheless, to date there are lack of the systematic efforts dedicating to the reaction mechanisms, isothermal curing kinetics, and properties of cured DGEBA/PAN4, and especially there remains a need for more comprehensive research to elucidate how the $-CH_2CH_2CN$ substituent on the amino groups of PAN4 affects the curing characteristics, thermal and bear-loading properties of the epoxy system. Such knowledge is important to better design and further guide better applications of acrylonitrile-modified dendritic polyamines curing agents.

In this work, we investigate the model-free isoconversional curing kinetics, dynamic mechanical properties, thermal decomposition, and mechanical properties of DGEBA/PAN4 and DGEBA/1.0GPPI in a systematic and comparative way. We shall elucidate how acrylonitrile-capped PAN4 affects the curing mechanisms, isothermal kinetics, processability, thermal, and dynamic and static mechanical properties of the resulting epoxy systems. Our current contribution will provide the comprehensive data to better understand properties of acrylonitrile-modified aliphatic amine curing agents, which is expected to be helpful for molecular design and further applications of aliphatic amine adduct curing agents.

2. Experimental

2.1. Materials

Ethylenediamine and acrylonitrile were purchased from Shanghai Reagent Co., Ltd., China, and were purified by reduced-pressure distillation. Propanediamine (Acros Organics) was used as received. Diglycidylether of bisphenol-A (DGEBA) (EEW = 196 g/equiv.) was obtained from Heli Resin Co., Ltd., China and dried at 100 °C in vacuum for 1 h before use. N,N,N′,N′-tetra(3-aminopropyl) ethanediamine (1.0GPPI) was prepared from ethylenediamine, acrylonitrile and H_2 according to published procedures [18,19]. The acrylonitrile-capped poly(propyleneimine) dendrimer (PAN4, CAS register number: 1267530-15-3) [17] has been synthesized in our laboratory for the first time. The molecular structures of DGEBA, 1.0GPPI and PAN4 are illustrated in Scheme 1.

2.2. DSC measurements

The nonisothermal curing reactions of DGEBA/1.0GPPI and DGEBA/PAN4 were followed by a PerkinElemer differential scanning calorimeter (DSC-7). All the DSC experiments were performed under N_2 protection, the scanning temperature was from 25 to 250 °C, and the heating rates were 5, 10, 15, and 20 °C min^{-1}. The

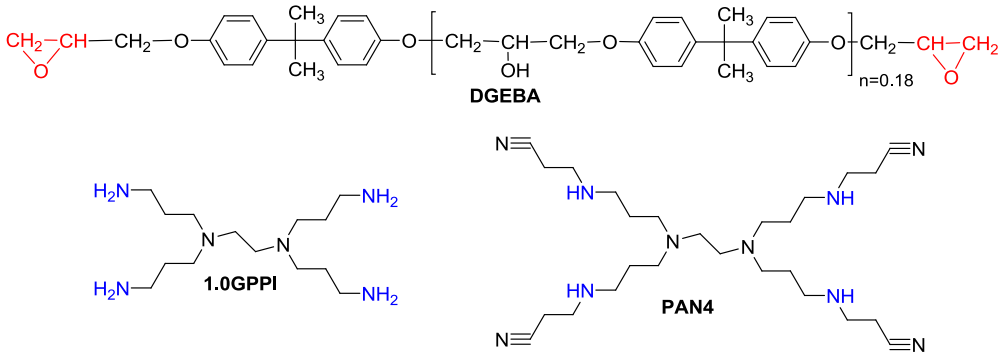

Scheme 1. Molecular structures of DGEBA, 1.0GPPI and PAN4.

nonisothermal heat flow as a function of temperature and time for the cure of DGEBA/1.0GPPI and DGEBA/PAN4 (epoxy group: amino hydrogen = 1:1 by mole) was illustrated in our previous publication [17].

2.3. Preparation of casting specimen

Stoichiometric DGEBA and 1.0GPPI, PAN4 or propanediamine were mixed well at room temperature and then poured into a preheated steeliness module. The module was transferred into an oven under reduced pressure for 5 min to drive off entrapped bubbles. The following temperature programs were used to finish the cure process in an air-blast oven: 70 °C/3 h + 150 °C/2 h for DGEBA/1.0GPPI and 80 °C/12 h for DGEBA/PAN4.

2.4. Property characterization

A dynamic mechanical analyzer (DMA Q800, TA instruments, USA) was used to examine the dynamic mechanical properties of the cured epoxy bars (dimension: 35 mm × 10 mm × 2 mm) with the heating rate of 3 °C min^{-1} from −100 °C to well above the glass temperature. The loading frequencies were 1, 3, 6, 12 and 24 Hz, the displacement amplitude was fixed as 15 μm, and the single cantilever clip was selected.

A thermogravimetric analyzer (PerkinElmer Pyris 1 TGA, USA) was used to analyze the thermal decomposition process of the cured epoxy. About 2–3 mg of the cured epoxy was subjected to thermogravimetric analysis under dynamic N_2 protection, and the heating rate was 10 °C min^{-1} with temperature ranging from 40 to 850 °C.

A Zwick/Roell Z020 Universal testing machine (Germany) was used to determine the flexural strengths of the cured epoxy specimen (dimension: 80 mm × 10 mm × 4 mm) according to GB T2570-1995 at 25 °C with the heading speed of 10 mm min^{-1}. The five specimens without bubbles were selected for the test.

A CEAST impact tester (Italy) was used to determine the Charpy impact strength of the cured epoxy specimens (dimension: 80 mm × 10 mm × 4 mm) in light of GB/T2567–1995 at 25 °C. The five specimens with a "V"-type notch were examined.

A Zwick/Roell Z020 universal testing machine was used to measure the shear strength of the epoxy-amine adhesives. To bonded substrate of two steel pieces (after cure at room temperature for 72 h), a vertical tensile stress was applied at the speed of 2 mm min^{-1} until rupture occurs. The shear strength was estimated in terms of $\tau = P/BL$ where τ is the shear strength, P is the maximum load applied to the bonded surface, and BL is the bonded surface area. The five parallel specimens were tested.

Gel time of the epoxy-amine reaction mixture was estimated at room temperature. The stoichiometric DGEBA and curing agent (about 5 g) were mixed homogenously in a test tube immersed in a constant-temperature water bath (25 °C). The recorded time for the reaction mixture to lose its macroscopic flow ability was considered as the gel time.

2.5. Fundamentals of model-free isoconversional analysis

The primary objectives of model-free isoconversional kinetic analysis are to estimate a dependence of effective activation energy on conversion and temperature, and further using this dependence makes kinetic predictions and exploring mechanisms of thermally stimulated physical or chemical processes [20]. The greatest advantage of such kind of kinetic analysis is general applicability without applying any specific kinetic models. For thermosets, optimal curing conditions depend strongly on reaction mechanisms and kinetics, so that accurately modeling cure is crucial [21]. More specifically, curing reactions of epoxy resins are highly exothermic because of ring opening of epoxy groups. In this case, registered DSC heat flow is assumed to be directly proportional to conversion of epoxy groups, as expressed by

$$\alpha = \frac{1}{\Delta H_o}\int_0^t \frac{dH}{dt}dt \tag{1}$$

where H is the DSC heat flow, t is the reaction time, and ΔH_o is the total reaction exotherm. Accordingly, reaction rate, $d\alpha/dt$, can be written as

$$\frac{d\alpha}{dt} = \frac{dH/dt}{\Delta H_o} = k(T)f(\alpha) \tag{2}$$

where $k(T)$ is the temperature-dependent rate constant. $k(T)$ follows the Arrhenius law.

$$k(T) = A\exp\left(-\frac{E_a}{RT}\right) \tag{3}$$

In Eq. (3), where A is the frequency factor, E_a is the activation energy, and R is the universal gas constant (8.314 J mol^{-1} K^{-1}).

Derivation of Eq. (2) with respect to $1/T$ yields Eq. (4):

$$\left[\frac{\partial \ln(d\alpha/dt)}{\partial T^{-1}}\right]_\alpha = \left[\frac{\partial \ln k(T)}{\partial T^{-1}}\right]_\alpha + \left[\frac{\partial \ln f(\alpha)}{\partial T^{-1}}\right]_\alpha \tag{4}$$

$f(\alpha)$ is the constant for given α, and thus Eq. (4) can be reduced to

$$\left[\frac{\partial \ln(d\alpha/dt)}{\partial T^{-1}}\right]_\alpha = \left[\frac{\partial \ln k(T)}{\partial T^{-1}}\right]_\alpha \tag{5}$$

On the basis of Eq. (5), a number of isoconversional methods have been developed, for example, the well-known Friedman [22], Flynn–Wall–Ozawa [23,24], Kissinger–Akahira–Sunose [25], and advanced isoconversional (Vyazovkin) [26–28] methods. In particular, due to its great accuracy and applicability to vast temperature programs, in this work the Vyazovkin method has been used to kinetic data analysis. To illustrate, for a thermal process carried out with multiple linear temperature programs, the Vyazovkin method can be expressed by

$$\Phi(E_\alpha) = \sum_{i=1}^{n}\sum_{j\neq i}^{n}\frac{I(E_\alpha, T_{\alpha,i})\beta_i^{-1}}{I(E_\alpha, T_{\alpha,j})\beta_i^{-1}} = \min \tag{6}$$

$$I(E_\alpha, T_{\alpha,i}) = \int_{T_{\alpha-\Delta\alpha}}^{T_\alpha} \exp\left[\frac{-E_\alpha}{RT_\alpha}\right]dT \tag{7}$$

where β_i and β_j represent the different heating rates, $\Delta\alpha$ is the conversion increment (usually 0.02), and T_α and $T_{\alpha-\Delta\alpha}$ are the reaction temperature for α and $\alpha - \Delta\alpha$, respectively. Minimizing Eq. (6) for each α will result in an $E_\alpha - \alpha$ correlation. Moreover, on the basis of E_α isothermal conversion can be predicated from the Vyazovkin equation [29,30]:

$$t_\alpha = \frac{\int_0^{T_\alpha}\exp\left(\frac{-E_\alpha}{RT_\alpha}\right)dT}{\beta\exp\left(\frac{-E_\alpha}{RT_{iso}}\right)} \tag{8}$$

where t_α is the reaction time for α and T_{iso} is the isothermal reaction temperature.

3. Results and discussion

3.1. Reactivity of DGEBA/1.0GPPI and DGEBA/PAN4

We examined the reactivity of curing agents, PAN4 and control 1.0GPPI, by using the nonisothermal DSC. Fig. 1 presents the representative heat flow–temperature curves of curing reactions of DGEBA/1.0GPPI and DGEBA/PAN4 with the heating rate of 5 °C min^{-1}, where the downward exothermic peak corresponds to the ring-opening reaction of epoxy groups under attack of amino groups. DGEBA/1.0GPPI shows the more extensive exothermic peak and much lower peak temperature than DGEBA/PAN4. The high exothermic peak temperature of DGEBA/PAN4 indicates that the acrylonitrile-substituted amino groups have the much low reactivity, because this substituent lowers the electron cloud density on nitrogen of the substituted amino groups due to the induction effect [17]. Moreover, the reaction heat estimated from the exothermic peaks is 510.8 J g^{-1} for DGEBA/1.0GPPI and 297.2 J g^{-1} for DGEBA/PAN4. The decreased exotherm of DGEBA/PAN4 results from the much high molecular weight but the half reduction in the functionalities of PAN4 ($f = 4$) as opposed to 1.0GPPI.

3.2. Effective activation energy of nonisothermal curing reactions

To examine the mechanisms of the curing reaction, the effective activation energy was determined and analyzed. Fig. 2 displays the curing curves of the fractional conversion as a function of the reaction temperature of DGEBA/1.0GPPI and DGEBA/PAN4 with the heating rates of 5, 10, 15 and 20 °C min^{-1}. These conversional curves exhibit the sigmoid profile, and the curves shift towards the higher temperature as the heating rate increased; i.e., the higher the heating rate, the higher the temperature for the reaction to reach the identical conversion. From Fig. 2, the effective activation energy was determined using the Vyazovkin method (Eqs. (6) and (7)).

As shown in Fig. 3, at the beginning of the curing reaction E_α decreases with α. This finding may result from the dramatic decrease in the viscosity with increasing temperature and the autocatalysis of the reaction, because these two effects lead to the decrease of the respective energetic barriers for the pure chemical reaction and the molecular diffusion. More interestingly, E_α of DGEBA/1.0GPPI is generally higher than that of DGEBA/PAN4 except for α higher than 0.9, which can be interpreted as follows. The $-CH_2CH_2CN$ substituent on the amino groups of PAN4 may lead to the decreased energetic barrier for the reacting intermediates of DGEBA/PAN4 by the dipole–dipole interaction (thus increasing the polarity of the reaction medium). On the other hand, when the reaction achieves the same conversion, the reaction temperature of DGEBA/PAN4 is much higher than that of DGEBA/1.0GPPI. In this case, the reaction intermediates of DGEBA/PAN4 may be more

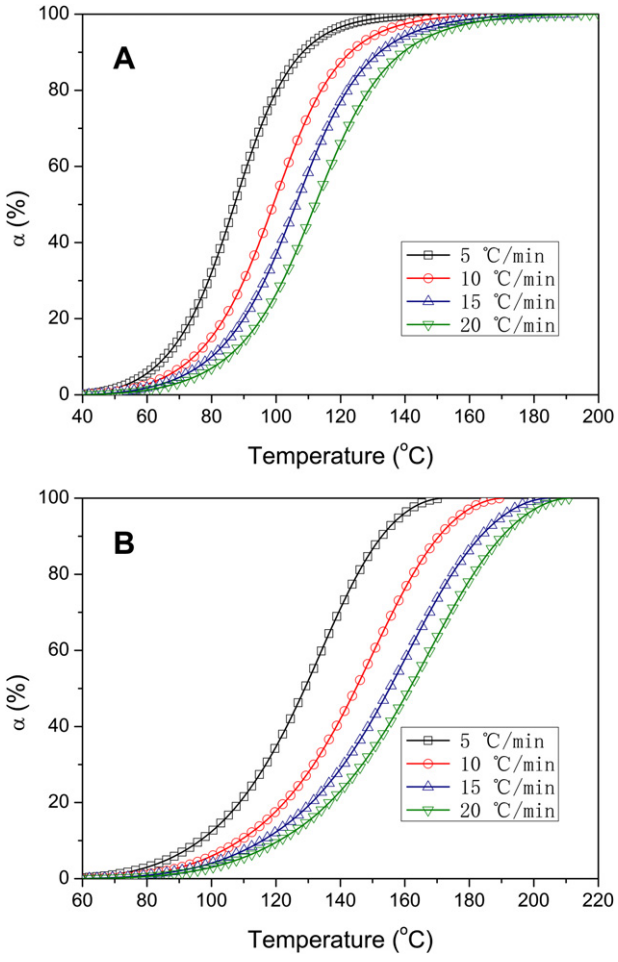

Fig. 2. Conversion of isothermal cure as a function of reaction temperature for different heating rates. (A) DGEBA/1.0GPPI and (B) DGEBA/PAN4.

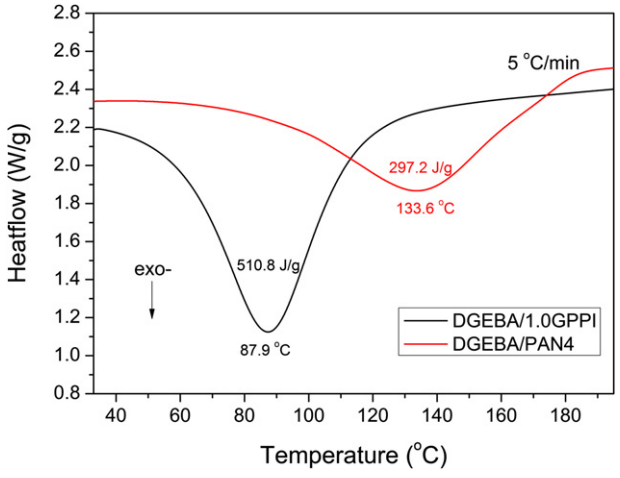

Fig. 1. Reprehensive DSC curves of nonisothermal curing reactions of DGEBA/1.0GPPI and DGEBA/PAN4 at heating rate of 5 °C min^{-1}.

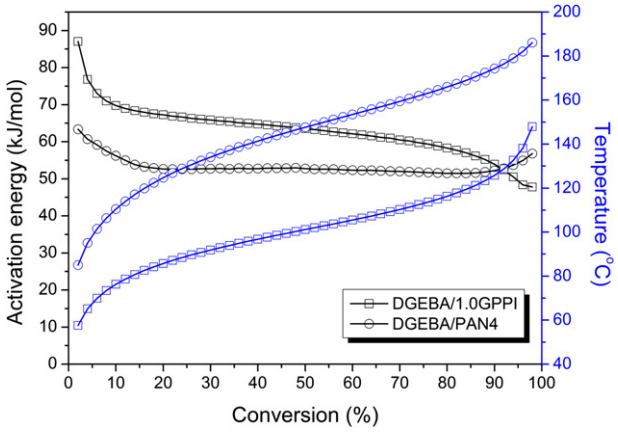

Fig. 3. Effective activation energy as a function of conversion and temperature for nonisothermal curing reactions of DGEBA/1.0GPPI and DGEBA/PAN4.

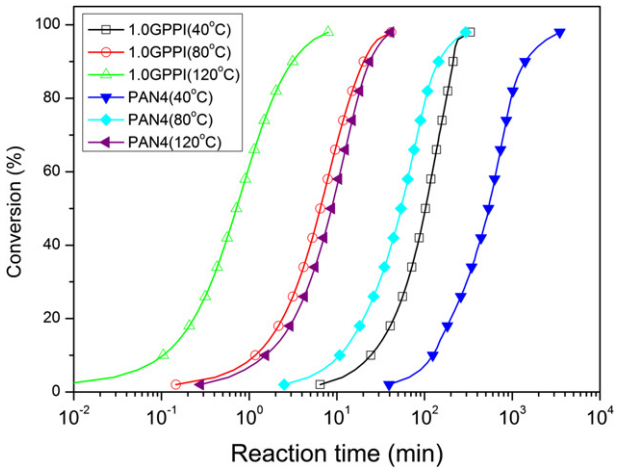

Fig. 4. Predicted conversion curves of curing reactions of DGEBA/1.0GPPI and DGEBA/PAN4 at 40, 80 and 120 °C.

sufficiently activated at the higher temperature. The dipole–dipole interaction and the higher reaction temperature of DGEBA/PAN4 lead to the lower energetic barriers for the curing reaction. As the reaction progresses into the deep-conversion stage, E_α of DGEBA/1.0GPPI tends to decrease, but that of DGEBA/PAN4 increases slightly. The former decrease can be attributed to the diffusion-associated reaction kinetics, because the reaction temperature is close to the glass temperature of the epoxy system. And the latter increase can be attributed to the etherification between the epoxy and hydroxyl groups, since in this conversion range the reaction temperature is rather high (>170 °C). In the intermediate conversion range ($0.2 < \alpha < 0.8$), E_α varies with α slightly, which may implicate that the influences of autocatalysis, viscosity, conversion, reaction temperature and other factors on the reaction kinetics achieve a quasi dynamic balance.

3.3. Isothermal kinetic prediction from nonisothermal data

The Vyazovkin equation (Eq. (8)) was used to predict the isothermal conversion of DGEBA/1.0GPPI and DGEBA/PAN4. Fig. 4 displays the predicated conversional curves for 40, 80 and 120 °C, and Table 1 compares the time for some typical conversions. The predicted data show that the reaction time of the two systems decreases systematically with the increased temperature, and 1.0GPPI reacts with DGEBA much faster than PAN4. For example, if the reaction temperature rises from 40 to 80–120 °C and when the two reactions reach the same conversion of 20%, the reaction time of DGEBA/1.0GPPI deceases from 44.8 to 2.4 to 0.23 min and that of DGEBA/PAN4 decreases from 199 to 20.2 to 3.2 min. The much longer reaction time of DGEBA/PAN4 is due to the appreciably decreased reactivity of PAN4 attributable to the electron-withdrawing effect of the $CNCH_2CH_2-$ substituent that causes the weakened nucleophilicity of the substituted amino groups towards

Table 1
Predicated reaction time to selected conversion for isothermal cure of DGEBA/1.0GPPI and DGEBA/PAN4 at 40, 80 and 120 °C.

Conversion (%)	DGEBA curing time for different temperatures (min)					
	40 °C		80 °C		120 °C	
	1.0GPPI	PAN4	1.0GPPI	PAN4	1.0GPPI	PAN4
20	44.8	199	2.4	20.2	0.23	3.2
50	102	536	6.5	54.0	0.71	8.7
80	178	968	14.1	103	1.9	17.3
98	333	3480	41.6	294	7.9	41.1

the epoxy rings by lowering the electron cloud density on the nitrogen of the amino groups. In addition, the $-CH_2CH_2CN$ substituent also increases the spatial hindrance of the substituted amino groups. Noticeably, the increased reaction time also suggests that PAN4 results in the resulting epoxy system with the much longer pot life, which will facilitate mixing and processing of resulting epoxy formulations greatly.

3.4. Viscoelastic relaxations and crosslink density of the cured epoxy

The viscoelastic relaxation and crosslink density of the cured epoxy network were examined from the dynamic mechanical analysis (DMA). Fig. 5 displays the reprehensive DMA spectra (1 Hz) for storage modulus E' and damping factor tan δ ($\delta = E''/E'$, where E'' is the loss modulus) vs. temperature for the two cured networks. DGEBA/1.0GPPI exhibits a slightly higher E' value than DGEBA/PAN4 at the lower temperature range; for instance, as shown in Table 2 at −100 °C E′ of the DGEBA/1.0GPPI and DGEBA/PAN4 networks is 6024 and 5922 MPa, respectively. These data demonstrate that although 1.0GPPI has the much lower molecular weight in combination with the doubled N–H functionalities leading to the more tightly crosslinked network, DGEBA/1.0GPPI still has close E' value compared with DGEBA/PAN4. This finding implicates that DGEBA/PAN4 has the stronger non-covalent bond interaction than DGEBA/1.0GPPI, especially at the low temperature range (<−100 °C). In addition, a small relaxation is observed below 0 °C and can be assigned to the β relaxation of the epoxy-amine networks associated with the local motions of the $-CH_2CH(OH)CH_2O-$ sequences [31–34]. In comparison, the β relaxation temperature T_β of DGEBA/PAN4 (−61.4 °C) is much lower than that of DGEBA/1.0GPPI (−34.5 °C). The lowered T_β is due to the decreased functionalities and increased molecular weight of PAN4 which lead to the much lower crosslink density of DGEBA/PAN4 network and thus the motions of the $-CH_2CH(OH)CH_2O-$ units become less restricted. In addition, DGEBA/PAN4 shows the much lower the altitude (peak height) than DGEBA/1.0GPPI, because of the decreased number of the $-CH_2CH(OH)CH_2O-$ units of DGEBA/PAN4 compared to DGEBA/1.0GPPI.

In an intermediate temperature range (−20 to 20 °C), DGEBA/PAN4 takes the higher E' value than DGEBA/1.0GPPI (Fig. 5). This observation contradicts with our common belief that the higher the crosslink density, the higher rigidity of the thermosetting networks exhibit. In fact, our finding is quite similar to a previous report [35] from the other epoxy-amine networks that the less crosslinked the epoxy-amine network, the higher modulus it showed in an ambient

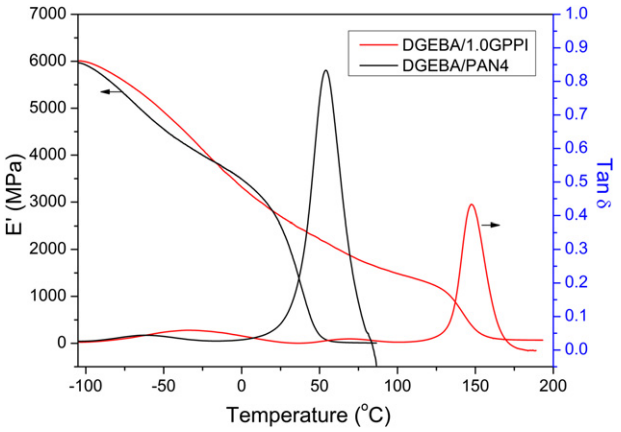

Fig. 5. Storage modulus E' and damping factor tan δ as a function of temperature. (1) DGEBA/1.0GPPI and (2) DGEBA/PAN4 networks at 1 Hz.

Table 2
Characteristic parameters (1 Hz) for relaxation of DGEBA/1.0GPPI, DGEBA/PAN4 and DGEBA/propanediamine (quoted from Ref. 8) networks.

	DGEBA/ 1.0GPPI	DGEBA/ PAN4	DGEBA/ propanediamine
α-relaxation (T_g)/°C	147.3	54.1	131.8
β-relaxation (T_β)/°C	−34.5	−61.4	−39.9
Modulus (−100 °C)/MPa	6024	5922	6044
Modulus (20 °C)/MPa	2811	2802	2860
Rubber modulus/MPa	67	13	37
Crosslink density/mol m^{-3}	5963	1459	3144

temperature range. The reason for our finding is as follows. The strong dipole–dipole interaction among the $-CH_2CH_2CN$ groups increases the cohesion energy density of the segments in DGEBA/PAN4 at the glass state, which results in the increased stiffness of the cured network. On the other hand, the β relaxation of DGEBA/1.0GPPI need invoke a larger number of the neighboring segments' cooperative motions compared to less crosslinked DGEBA/PAN4, so that we observe that the higher damping (loss of storage elastic energy) occurs during the β relaxation associated with plastic deformation of the DGEBA/1.0GPPI network. Collectively, the dipole–dipole interaction and the damping associated with the β relaxation cause that the E' value of DGEBA/PAN4 surpasses that of DGEBA/1.0GPPI in this temperature range.

As the temperature further increases, E' of the networks drops sharply from over 1000 MPa to below 100 MPa, while Tan δ goes through the maximum. These observations are indicative of the glass-rubber relaxation of the networks arising from the cooperative motions of the whole network chains. The data in Table 2 show that DGEBA/PAN4 has much lower T_g for Tan δ_{max} (54.1 °C) than DGEBA/1.0GPPI (147.3 °C). Decreased T_g is associated with the dangling $-CH_2CH_2CN$ segments from PAN4 which increase the average chain length and in turn decrease the crosslink density of the DGEBA/PAN4 network. What is more, the $-CH_2CH_2CN$ segments, functioning as the chain ends, may increase the free volume of the network. Fig. 5 also shows that the glass relaxation temperature range of the DGEBA/PAN4 network is broader and the altitude is higher (Tan $\delta_{max} > 0.8$) in comparison with DGEBA/1.0GPPI. This phenomenon results from the boarder chain distribution of the DGEBA/PAN4 network. Note here that such high Tan δ near the room temperature range likely manifests the promise of DGEBA/PAN4 for room-temperature damping materials [36].

At the rubbery state, the two networks manifest very small E' with the plateau value of a few dozens of mega pascals, and the rubbery modulus E_r is taken as E' for $T_g + 30$ °C. As shown in Table 2, DGEBA/1.0GPPI has a much higher E_r (67 MPa) than DGEBA/PAN4 (13 MPa), which is associated with the much difference in crosslink density of the networks. From E_r, the crosslink density ν_e can be estimated using Eq. (9) [36–39]:

$$\nu_e = \frac{E_r}{3RT_r} \tag{9}$$

where T_r is the absolute temperature (K) for E_r and R is the universal gas constant. As seen in Table 2, DGEBA/1.0GPPI has much higher ν_e than DGEBA/propanediamine (3144 mol m^{-3}), and the reason is that 1.0GPPI has the branched molecular structure, which in turn lead to the additional crosslinks in the network. Moreover, DGEBA/PAN4 exhibits the much lower ν_e value than DGEBA/1.0GPPI (1459 vs. 5963 mol m^{-3}), largely because of the decreased number of the N–H functionalities and increased molecular weight of PAN4. Another contributing factor is the $-CH_2CH_2CN$ segments that increase the free volume of the network by increasing the number of the chain ends, which may partiality respond for decreased E_r and thus ν_e. Note that the $-CH_2CH_2CN$ segments contribute to the high E' value of DGEBA/PAN4 via the strong dipole–dipole interaction when the network is at the glassy sate, whereas in the rubbery state they affect E' negatively due to the decreased number of crosslink density. To illustrate, at the rubbery state, the network chains have processed enough kinetic energy to eliminate the influence of the dipole–dipole force (the non-covalent bond interaction) among the $-CH_2CH_2CN$ segments. In this case, the crosslink density is more important in determining the stiffness of the network instead of the non-covalent segment interaction.

3.5. Relaxation activation energy

Activation energy is an important parameter for characterizing viscoelastic responses of polymer networks, and its value can be calculated from the Arrhenius equation [36–44]; see Eqs. (10)–(11):

$$f = f_0 \exp\left(\frac{E}{RT}\right) \tag{10}$$

$$E = -R\left[\frac{d(\ln f)}{d(1/T_R)}\right] \tag{11}$$

where f is the frequency, f_0 is the pre-exponential factor, E is the relaxation activation, R is the gas constant (8.314 J mol^{-1} K^{-1}), and T_R is the relaxation temperature. According to Eq. (11), a set of dynamic mechanical measurements at different frequencies need carrying out to result in a set of f–T_R data, and then linearly fitting $\ln f$ with respect to $1/T_R$ gives rise to E value.

Here a multi-frequency DMA technique was used to determine the relaxation activation energy of the DGEBA/PAN4 and DGEBA/1.0GPPI networks. Fig. 6 displays the plots of Tan δ against the temperature for f of 1, 3, 6, 12 and 24 Hz, from which the relaxation is found to shift towards a higher temperature as f increases. Accordingly, Table 3 lists the relaxation temperatures for Tan δ, T_α and T_β, and the corresponding temperatures for loss modulus E''. The data demonstrate that T_α and T_β increase systematically with increased f, but the amplitude changes slightly. The β relaxation temperatures seem more sensitive to f compared to the α-relaxation, which is likely associated with the difference in the activation energy for the two relaxations.

From the data in Table 3, a plot of $\ln f$ against $1/T_R$ is constructed in Fig. 7. The slopes of the fitted straight lines give rise to the activation energy for the α and β relaxations; see Table 4. Note here that the plot of $1/T_{loss}$ (for loss modulus) against $\ln f$ yields a relatively poor linear correlation, especially for the α relaxation, which is similar to the result from the other epoxy-amine networks [41]. Thus, it is more reasonable to use $T_{\tan\delta}$–f data to estimate E_α and E_β, and the data are shown in Table 4.

E_α is much higher than the corresponding E_β, which can support the motions of the whole network chains. The cooperative motions of the segments need much higher energetic energy than the localized motions of the $-CH_2CH(OH)CH_2O-$ segments. By comparison, E_α of DGEBA/1.0GPPI is more than two times that of DGEBA/PAN4, which can be attributed to the dramatic change in the crosslink density of the two networks. The much more crosslinked DGEBA/1.0GPPI network makes the cooperative motions of the chains much more restricted, so that a larger number of the segments have to be invoked during the glass relaxation process, eventually leading to the higher glass-relaxation activation energy. Despite of that, DGEBA/1.0GPPI shows only slightly higher E_β value than that of DGEBA/PAN4, and this value is also comparable to several other epoxy-amine networks [35,40]. This similarity suggests that the crosslink density has little influence on the fundamental molecular mechanism for the β relaxation. In other words, the relaxation mechanisms of the $-CH_2CH(OH)CH_2O-$ sequences less depend upon the crosslink density, because the chain motions involved in the β relaxation are restricted in a very

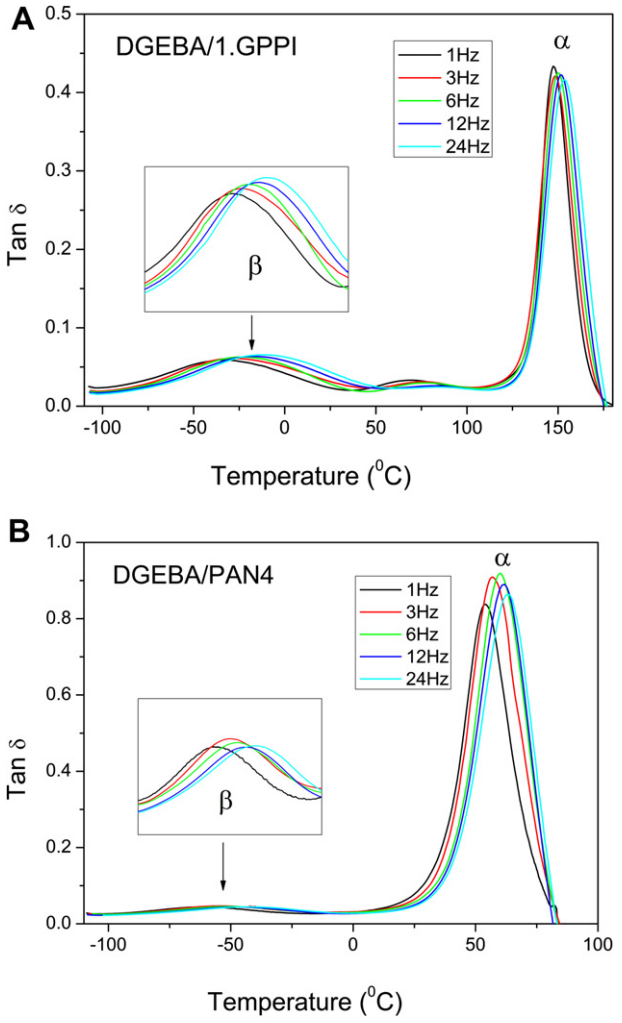

Fig. 6. Tan δ-temperature curve for cured DGEBA/1.0GPPI and DGEBA/PAN4 networks with oscillation frequency of 1, 3, 6, 12 and 24 Hz.

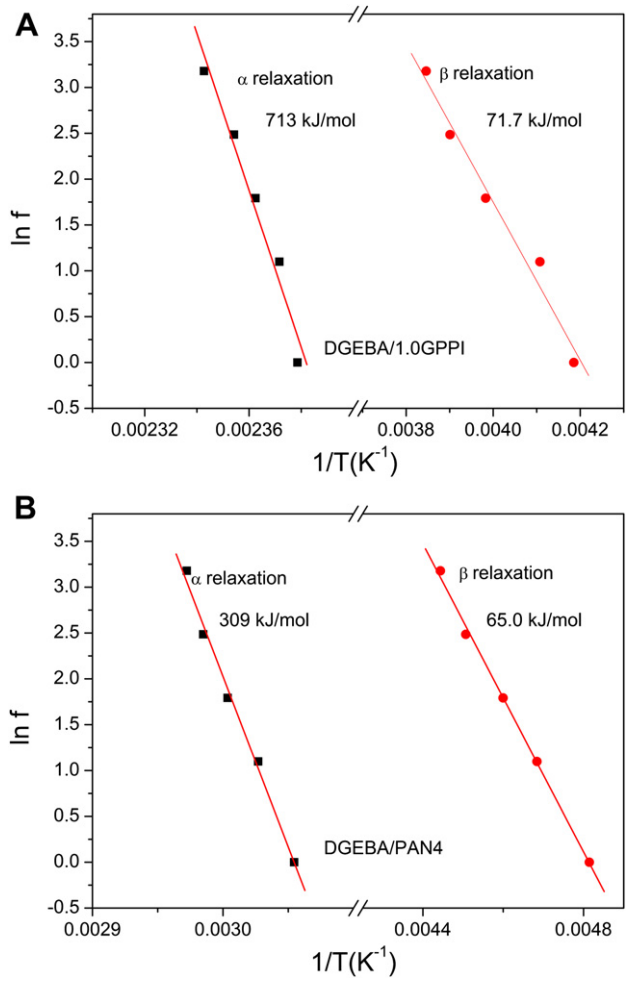

Fig. 7. Arrhenius plots of ln f against $1/T$ for DGEBA/1.0GPPI and DGEBA/PAN4 networks.

short range, which needs only a slight cooperation of the surrounding chains.

3.6. Relaxation activation enthalpy and entropy

Relaxation activation energy E can be separated into terms of activation entropy $\Delta H^{\dagger}$ and activation enthalpy $\Delta S^{\dagger}$ according to the absolute rate equation (Eq. (12)), and the derived expressions for $\Delta H^{\dagger}$ and $\Delta S^{\dagger}$ can be expressed as Eqs. (13) and (14) [35,45–48], respectively.

$$f = (kT/2\pi h)\exp(-\Delta H^{\dagger}/RT)\exp(\Delta S^{\dagger}/R) \quad (12)$$

$$\Delta H^{\dagger} = E - RT' \quad (13)$$

$$\Delta S^{\dagger} = \frac{E - RT'[1 + \ln(kT'/2\pi h)]}{T'} \quad (14)$$

In these equations T' is the temperature at which E'' arrives at the maximum (1 Hz) as shown in Fig. 8, h is the Planck constant (6.626×10^{-34} J s), and k is the Boltzmann constant (1.38×10^{-23} J K^{-1}).

$\Delta H^{\dagger}$ and $\Delta S^{\dagger}$ estimated from Eqs. (13) and (14) are shown in Table 5. $\Delta H^{\dagger}$ is fairly close to the corresponding E, resembling the case of other epoxy-amine networks [35]. More interestingly, although $\Delta S^{\dagger}$ for the β relaxation of the two networks differs slightly, the α relaxation of DGEBA/1.0GPPI takes the higher $\Delta S^{\dagger}$

Table 3
α and β relaxation temperatures for DGEBA/1.0GPPI and DGEBA/PAN4 networks at different frequencies.

f (Hz)	DGEBA/1.0GPPI (°C)				DGEBA/PAN4 (°C)			
	$T_{\alpha,\tan\delta}$	$T_{\alpha,\mathrm{loss}}$	$T_{\beta,\tan\delta}$	$T_{\beta,\mathrm{loss}}$	$T_{\alpha,\tan\delta}$	$T_{\alpha,\mathrm{loss}}$	$T_{\beta,\tan\delta}$	$T_{\beta,\mathrm{loss}}$
1	147.3	141.3	−34.5	−43.2	54.1	38.4	−61.4	−65.4
3	148.5	140.8	−28.3	−40.6	57.2	41.5	−54.8	−59.5
6	150.1	142.1	−23.3	−34.4	59.8	44.3	−50.4	−55.6
12	151.6	143.4	−17.4	−28.1	61.9	44.7	−47.4	−51.1
24	153.7	145.1	−13.1	−22.2	63.3	46.5	−42.4	−48.1

Table 4
Activation energies for α and β relaxations of DGEBA/1.0GPPI and DGEBA/PAN4 networks. Tan δ and E'' indicate the relaxation activation energies calculated from the damping and loss modulus peak temperatures, respectively.

		E_{α} kJ mol^{-1}	E_{β} kJ mol^{-1}	R_{α}	R_{β}
DGEBA/1.0GPPI	Tan δ	713	71.7	−0.984	−0.987
	E''	657	37.6	−0.879	−0.975
DGEBA/PAN4	Tan δ	309	65.0	−0.995	−0.994
	E''	311	69.9	−0.983	−0.997

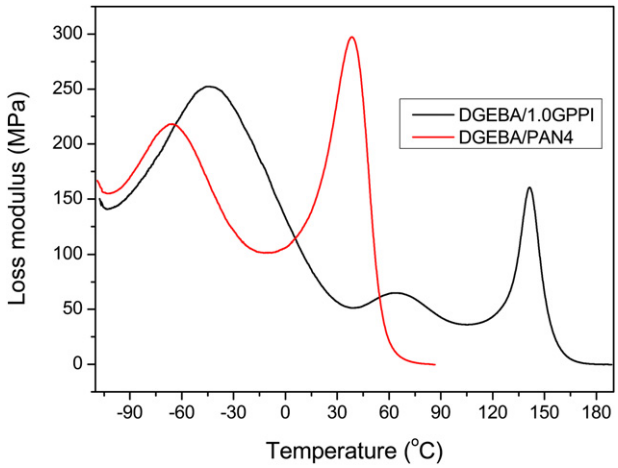

Fig. 8. Loss modulus E'' as a function of temperature for DGEBA/1.0GPPI and DGEBA/PAN4 networks (1 Hz).

value than that of DGEBA/PAN4. The reason may be that the increased crosslink density leads to the increased number of the cooperative segments motions during the α relaxation, whereas the localized motions of the $-CH_2CH(OH)CH_2O-$ sequences could trigger the very limited cooperative movement of the neighboring segments. However, in other epoxy-amine networks [35], $\Delta S^{\dagger}$ for the β relaxation was found to increase with increased crosslink density, which was attributed to more restricted surrounding of the $-CH_2CH(OH)CH_2O-$ segments. This contradicted observation likely indicates that a compensation mechanism for $\Delta S^{\dagger}$ may exist in the DGEBA/PAN4 network when considering its much lowered crosslink density. The reasons are as follows. At the lower temperature the configuration rearrangement of the molecular chains is to some extent restricted by the strong dipole–dipole interaction among the $-CH_2CH_2CN$ groups, and thus $\Delta S^{\dagger}$ for the β relaxation of DGEBA/PAN4 increases. On the other hand, the higher crosslink density of the DGEBA/1.0GPPI network is expected to respond for increased $\Delta S^{\dagger}$, but the intermolecular interaction in this network is not as strong as that in the DGEBA/PAN4 network for the β relaxation. For the α relaxation, on the other hand, DGEBA/1.0GPPI has much higher $\Delta H^{\dagger}$ and $\Delta S^{\dagger}$ than DGEBA/PAN4, which quite differs from the case of the β relaxation. The higher $\Delta H^{\dagger}$ and $\Delta S^{\dagger}$ values for the α relaxations of the networks substantiate that the α relaxation needs much higher kinetic energy than the β relaxation and result in the much higher disorder in the networks after the α relaxation. Noticeably, the very high $\Delta H^{\dagger}$ and E values for the α relaxations likely implicate the complex microscopic molecular relaxation mechanisms of the glass relaxation.

3.7. Thermal decomposition behavior

Fig. 9A presents the TG thermographs of cured DGEBA/PAN4 and DGEBA/1.0GPPI. The result illustrates that DGEBA/1.0GPPI has the excellent thermal stability up to 270 °C (for 0.5% mass loss), whereas DGEBA/1.0GPPI is thermally stable up to 200 °C. These data suggest that 1.0GPPI and PAN4 can endow the cured epoxy with sufficiently high thermal stability for room temperature applications such as coatings and adhesives. From Fig. 9B where the curves of the thermal decomposition rate vs. temperature are presented, DGEBA/1.0GPPI shows a single peak that can be assigned to the random rupture of the network chains. This observation differs greatly from what is found from DGEBA/PAN4, where the two-step thermal decomposition kinetic schemes can be clearly identified. The first step appears at the lower temperature with the peak temperature of ≈250 °C and the other at the higher temperature with the peak temperature of ≈400 °C. Moreover, DGEBA/PAN4 loses the ≈16% original mass at 300 °C (Fig. 9A), which is close to the fraction (≈14%) calculated from the $-CH_2CH_2CN$ substituent from acrylonitrile in the epoxy system. This agreement indicates the thermal decomposition of DGEBA/PAN4 at the relatively low temperature is due to the detachment of the $-CH_2CH_2CN$ moieties from the cured epoxy via the *retro*-Michael addition mechanism [49]. At the higher temperature range, the decomposition of DGEBA/PAN4 results from the random scission of the residual.

Fig. 9A also indicates DGEBA/PAN4 exhibits the lower residual char yield than DGEBA/1.0GPPI after the high-temperature pyrolysis, suggesting the detachment of $-CH_2CH_2CN$ moieties promotes the further thermal decomposition of the cured epoxy resin matrix. For example, the lower crosslink density of the DGEBA/PAN4 network renders the easier departure of the volatile products at the higher temperature. After the thermal scission of the $-CH_2CH_2CN$ moieties, the further liberation of volatile gaseous products becomes easier during the higher-temperature pyrolysis, since the surface area of the pyrolyzate is likely much increased after the first stage of the thermal degradation. Furthermore, the fraction of the aromatic moieties is decreased due to the much increased stoichiometry of the reactive amino hydrogen (N–H) of PAN4 (125 g mol^{-1}) compared to 1.0GPPI (30.4 g mol^{-1}), which partially responds for the decreased yield for DGEBA/PAN4. In summary, the introduction of the $-CH_2CH_2CN$ moieties into the DGEBA/PAN4 system moderately decreases the thermal stability, but the cured epoxy still has the high enough thermal stability to satisfy the room temperature applications.

3.8. Mechanical properties and gel time

To further investigate the other properties of PAN4, in Table 6 we compared the flexural, impact, shear strengths and the gel time of the propanediamine-, 1.0GPPI- and PAN4-cured epoxy systems. DGEBA/1.0GPPI and DGEBA/propanediamine have the comparable flexural strength, but the former exhibits the lower impact strength and shorter gel time. The decreased impact strength is owing to the higher crosslink density of DGEBA/1.0GPPI, which causes the less elastic deformation of the network before rupture. On the other hand, the shortened gel time is due largely to the doubled N–H functionalities of 1.0GPPI compared to propanediamine (8 *vs.* 4). Interestingly, DGEBA/1.0GPPI shows the much higher shear strength than DGEBA/propanediamine. This finding is likely associated with the stronger adhesion between the cured epoxy matrix and bonded steel surface, since the tertiary amino groups from

Table 5
Activation enthalpy $\Delta H^{\dagger}$, entropy $\Delta S^{\dagger}$, and temperature for peak loss modulus (1 Hz) T_{loss} of DGEBA/1.0GPPI and DGEBA/PAN4 networks.

	α Relaxation			β Relaxation		
	$\Delta H^{\dagger}$ kJ mol^{-1}	$\Delta S^{\dagger}$ J K^{-1} mol^{-1}	T_{loss} °C	$\Delta H^{\dagger}$ kJ mol^{-1}	$\Delta S^{\dagger}$ J K^{-1} mol^{-1}	T_{loss} °C
DGEBA/1.0GPPI	709	1630	141.3	69.8	222	−43.2
DGEBA/PAN4	306	902	38.4	63.3	223	−65.4

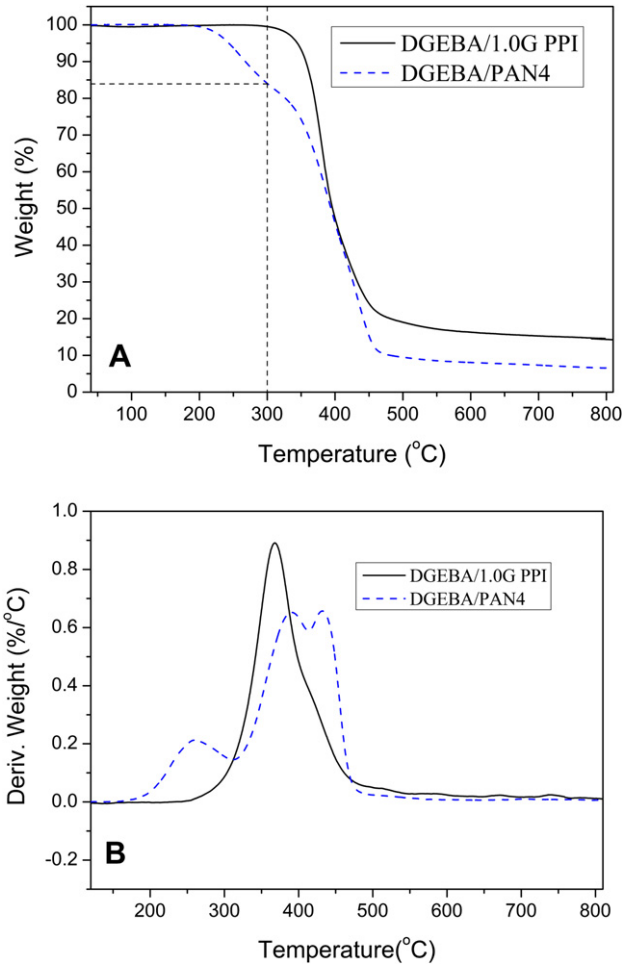

Fig. 9. TG and DTG thermographs of cured DGEBA/1.0GPPI and DGEBA/PAN4 in N_2 (10 °C min^{-1}).

1.0GPPI are expected to able to more tightly associate with ferrous atoms at the bonded surface.

Compared to DGEBA/propanediamine and DGEBA/1.0GPPI, the flexural strength of DGEBA/PAN4 is decreased by about half, because of the much decreased crosslink density of the DGEBA/PAN4 network. The decreased crosslink density even leads to the yielding of DGEBA/PAN4 before rupture. Impressively, the impact strength, shear strength and gel time of DGEBA/PAN4 are increased by several folds compared to the other two systems. The enhancement in the impact strength can be attributed to the increased molecular mobility which causes the much higher impact energy being dissipated via the plastic deformation mechanism before rupture. On the other hand, the dramatically increased shear strength of DGEBA/PAN4 is owing to the $-CH_2CH_2CN$ substituent of PAN4. The $-CH_2CH_2CN$ substituent is expected to produce the much stronger adhesion at the bonded surface because of the strong interaction between the ferrous atoms and $-CH_2CH_2CN$ groups (somewhat like a coordination bond between ferrum and nitrile group). Moreover, the $-CH_2CH_2CN$ substituent decreases the reactivity and functionality of PAN4, and thus leads to the much longer gel time of DGEBA/PAN4 (Table 6), which will lead to the better wetting between the epoxy matrix and steel surface. Furthermore, the cured DGEBA/PAN4 network is much ductile, which improves the stress transfer at the interface and thus releases the stress concentration. Also, the much longer gel time of DGEBA/PAN4 indicates the excellent processability of the resulting epoxy formulation for the room-temperature applications. To summarize, PAN4 endows the resulting epoxy system with the excellent impact strength, shear strength, and much longer pot life compared with 1.0GPPI and conventional aliphatic-amine curing agents like propanediamine. Due to these merits, PAN4 may be suitable for a new epoxy curing agent for room temperature applications.

Table 6
Mechanical properties and gel time of DGEBA/1.0GPPI, DGEBA/PAN4, DGEBA/propanediamine systems.

	Flexural strength	Impact strength	Shear strength	Gel time at 25 °C
	MPa	kJ m^{-2}	MPa	min
DGEBA/propanediamine	102.0 ± 6.1	3.2 ± 0.7	2.4 ± 0.4	170–190
DGEBA/1.0GPPI	96.8 ± 4.3	2.3 ± 0.7	4.0 ± 0.4	130–150
DGEBA/PAN4	51.8 ± 2.3[a]	9.8 ± 1.5	16.1 ± 1.0	>720

[a] Here the flexural strength was taken as the yield strength of the material.

4. Conclusions

We have systematically investigated the model-free isoconversional nonisothermal curing kinetics, thermal decomposition, and mechanical properties of DGEBA/PAN4 and controlled DGEBA/1.0GPPI. DGEBA/PAN4 showed the lower reactivity and reaction heat than DGEBA/1.0GPPI. The model-free isoconversional kinetic analysis revealed that effective activation energy E_α varied substantially with conversion α, and DGEBA/PAN4 had generally lower E_α than DGEBA/1.0GPPI. The isothermal conversion was predicted from the dynamic cure by using the Vyazovkin equation, and the simulated data suggested that PAN4 reacted with DGEBA far lower than 1.0GPPI. The subsequent dynamic mechanical analysis of the cure epoxy revealed that compared with DGEBA/1.0GPPI, DGEBA/PAN4 showed the lower β- and α-relaxation temperatures, much lower crosslink density, but the much higher damping near room temperature. Furthermore, the multiple-frequency dynamic mechanical analysis of the cured epoxy networks demonstrated that DGEBA/PAN4 had the lower relaxation activation energy, enthalpy and entropy values for the α relaxation than the controlled DGEBA/1.0GPPI. Nevertheless, the corresponding values for the β relaxation of the two networks differed slightly owing to the strong dipole–dipole interaction among the $-CH_2CH_2CN$ groups of the DGEBA/PAN4 network at its glass state, which may compensate the negative influence of the lower crosslink density. Then, the thermogravimetric analysis demonstrated DGEBA/PAN4 was thermally stable up to 200 °C, and the decomposition process followed the two-step kinetic schemes: the initial detachment of the $-CH_2CH_2CN$ and the further decomposition of the networks. Finally it turned out experimentally that PAN4 endowed the cured epoxy resins with the very long gel time, much higher impact resistance, and much stronger shear strength. From the analyses above, we can generalize that PAN4 has a great potential as a new curing agent for high-performance room-temperature epoxy adhesives, coatings, and even damping materials.

Acknowledgments

Our particular recognition is due to the financial support of work by the Postdoctoral Foundation of Zhejiang Province, China (Grant No. Bsh1201004) and the Program for Changjiang Scholars and Innovative Research Team in University, China (PCSIRT). We would like to appreciate the referees for giving us the helpful comments.

References

[1] A.T. Seyhan, Z. Sun, J. Deitzel, M. Tanoglu, D. Heider, Cure kinetics of vapor grown carbon nanofiber (VGCNF) modified epoxy resin suspensions and

fracture toughness of their resulting nanocomposites, Mater. Chem. Phys. 118 (2009) 234–242.
[2] J. Qiu, S. Wang, Reaction kinetics of functionalized carbon nanotubes reinforced polymer composites, Mater. Chem. Phys. 121 (2010) 295–301.
[3] H. Liu, Z.-e. Fu, K. Xu, H.-l. Cai, X. Liu, M.-C. Chen, Preparation and characterization of high performance Schiff-base liquid crystal diepoxide polymer, Mater. Chem. Phys. 132 (2012) 950–956.
[4] F.-X. Perrin, T.M.H. Nguyen, J.-L. Vernet, Kinetic analysis of isothermal and nonisothermal epoxy-amine cures by model-free isoconversional methods, Macromol. Chem. Phys. 208 (2007) 718–729.
[5] F.X. Perrin, T.M.H. Nguyen, J.L. Vernet, Chemico-diffusion kinetics and TTT cure diagrams of DGEBA-DGEBF/amine resins cured with phenol catalysts, Eur. Polym. J. 43 (2007) 5107–5120.
[6] O. Zabihi, A. Hooshafza, F. Moztarzadeh, H. Payravand, A. Afshar, R. Alizadeh, Isothermal curing behavior and thermo-physical properties of epoxy-based thermoset nanocomposites reinforced with Fe_2O_3 nanoparticles, Thermochim. Acta 527 (2012) 190–198.
[7] O. Zabihi, A. Khodabandeh, S. Ghasemlou, Investigation of mechanical properties and cure behavior of DGEBA/nano-Fe_2O_3 with polyamine dendrimer, Polym. Degrad. Stab. 97 (2012) 1730–1736.
[8] J. Wan, C. Li, Z.-Y. Bu, C.-J. Xu, B.-G. Li, H. Fan, A comparative study of epoxy resin cured with a linear diamine and a branched polyamine, Chem. Eng. J. 188 (2012) 160–172.
[9] J. Wan, Z.-Y. Bu, C.-J. Xu, B.-G. Li, H. Fan, Preparation, curing kinetics, and properties of a novel low-volatile starlike aliphatic-polyamine curing agent for epoxy resins, Chem. Eng. J. 171 (2011) 357–367.
[10] J. Wan, Z.-Y. Bu, C.-J. Xu, H. Fan, B.-G. Li, Model-fitting and model-free nonisothermal curing kinetics of epoxy resin with a low-volatile five-armed starlike aliphatic polyamine, Thermochim. Acta 525 (2011) 31–39.
[11] J. Wan, B.-G. Li, H. Fan, Z.-Y. Bu, C.-J. Xu, Nonisothermal reaction, thermal stability and dynamic mechanical properties of epoxy system with novel nonlinear multifunctional polyamine hardener, Thermochim. Acta 511 (2010) 51–58.
[12] J. Wan, B.-G. Li, H. Fan, Z.-Y. Bu, C.-J. Xu, Nonisothermal reaction kinetics of DGEBA with four-armed starlike polyamine with benzene core (MXBDP) as novel curing agent, Thermochim. Acta 510 (2010) 46–52.
[13] Y. Cheng, T. Xu, P. He, Polyamidoamine dendrimers as curing agents: the optimum polyamidoamine concentration selected by dynamic torsional vibration method and thermogravimetric analyses, J. Appl. Polym. Sci. 103 (2007) 1430–1434.
[14] Y. Cheng, D. Chen, R. Fu, P. He, Behavior of polyamidoamine dendrimers as curing agents in bis-phenol A epoxy resin systems, Polym. Int. 54 (2005) 495–499.
[15] D.-M. Xu, K.-D. Zhang, X.-L. Zhu, Curing of DGEBA epoxy resin by low generation amino-group-terminated dendrimers, J. Appl. Polym. Sci. 101 (2006) 3902–3906.
[16] J. Wan, Z.-Y. Bu, C.-J. Xu, B.-G. Li, H. Fan, Learning about novel amine-adduct curing agents for epoxy resins: butyl-glycidylether-modified poly(-propyleneimine) dendrimers, Thermochim. Acta 519 (2011) 72–82.
[17] J. Wan, H. Fan, B.-G. Li, C.-J. Xu, Z.-Y. Bu, Synthesis and nonisothermal reaction of a novel acrylonitrile-capped poly(propyleneimine) dendrimer with epoxy resin, J. Therm. Anal. Calorim. 103 (2011) 685–692.
[18] M.M.d.B.-v.d.B. Ellen, E.W. Meijer, Poly(propylene imine) dendrimers: large-scale synthesis by hetereogeneously catalyzed hydrogenations, Angew. Chem. Int. Ed. Engl. 32 (1993) 1308–1311.
[19] C. Wörner, R. Mülhaupt, Polynitrile- and polyamine-functional poly(trimethylene imine) dendrimers, Angew. Chem. Int. Ed. Engl. 32 (1993) 1306–1308.
[20] S. Vyazovkin, N. Sbirrazzuoli, Isoconversional kinetic analysis of thermally stimulated processes in polymers, Macromol. Rapid Commun. 27 (2006) 1515–1532.
[21] M. Sultania, J.S.P. Rai, D. Srivastava, Modeling and simulation of curing kinetics for the cardanol-based vinyl ester resin by means of non-isothermal DSC measurements, Mater. Chem. Phys. 132 (2012) 180–186.
[22] H.L. Friedman, Kinetics of thermal degradation of char-forming plastics from thermogravimetry. Application to a phenolic plastic, J. Polym. Sci. Part C Polym. Symp. 6 (1964) 183–195.
[23] J.H. Flynn, L.A. Wall, General treatment of the thermogravimetry of polymers, J. Res. Natl. Bur. Stand. A. Phys. Chem. A. Phys. Chem. 70A (1966) 487–523.
[24] T. Ozawa, A new method of analyzing thermogravimetric data, Bull. Chem. Soc. Jpn. 38 (1965) 1881–1886.
[25] T. Akahira, T. Sunose, Method of determining activation deterioration constant of electrical insulating materials, Res. Rep. Chiba Inst. Technol. (Sci. Technol.) 16 (1971) 22–31.
[26] S. Vyazovkin, D. Dollimore, Linear and nonlinear procedures in isoconversional computations of the activation energy of nonisothermal reactions in solids, J. Chem. Inf. Comput. Sci. 36 (1996) 42–45.
[27] S. Vyazovkin, Evaluation of activation energy of thermally stimulated solid-state reactions under arbitrary variation of temperature, J. Comput. Chem. 18 (1997) 393–402.
[28] S. Vyazovkin, Modification of the integral isoconversional method to account for variation in the activation energy, J. Comput. Chem. 22 (2001) 178–183.
[29] S. Vyazovkin, Model-free kinetics staying free of multiplying entities without necessity, J. Therm. Anal. Calorim. 83 (2006) 45–51.
[30] S. Vyazovkin, A.K. Burnham, J.M. Criado, L.A. Pérez-Maqueda, C. Popescu, N. Sbirrazzuoli, ICTAC kinetics committee recommendations for performing kinetic computations on thermal analysis data, Thermochim. Acta 520 (2011) 1–19.
[31] O. Delatycki, J.C. Shaw, J.G. Williams, Viscoelastic properties of epoxy-diamine networks, J. Polym. Sci. Part B Polym. Phys. 7 (1969) 753–762.
[32] S.A. Paipetis, P.S. Theocaris, A. Marchese, The dynamic properties of plasticized epoxies over a wide frequency range, Colloid Polym. Sci. 257 (1979) 478–485.
[33] M. Ochi, M. Okazaki, M. Shimbo, Mechanical relaxation mechanism of epoxide resins cured with aliphatic diamines, J. Polym. Sci. Part B Polym. Phys. 20 (1982) 689–699.
[34] G.W. John, The beta relaxation in epoxy resin-based networks, J. Appl. Polym. Sci. 23 (1979) 3433–3444.
[35] S. Cukierman, J.-L. Halary, L. Monnerie, Dynamic mechanical response of model epoxy networks in the glassy state, Polym. Eng. Sci. 31 (1991) 1476–1482.
[36] A. Shabeer, A. Garg, S. Sundararaman, K. Chandrashekhara, V. Flanigan, S. Kapila, Dynamic mechanical characterization of a soy based epoxy resin system, J. Appl. Polym. Sci. 98 (2005) 1772–1780.
[37] F. Fernandez-Nograro, A. Valea, R. Llano-Ponte, I. Mondragon, Dynamic and mechanical properties of DGEBA/poly(propylene oxide) amine based epoxy resins as a function of stoichiometry, Eur. Polym. J. 32 (1996) 257–266.
[38] J.S. Nakka, K.M.B. Jansen, L.J. Ernst, W.F. Jager, Effect of the epoxy resin chemistry on the viscoelasticity of its cured product, J. Appl. Polym. Sci. 108 (2008) 1414–1420.
[39] A. Gerbase, C. Petzhold, A. Costa, Dynamic mechanical and thermal behavior of epoxy resins based on soybean oil, J. Am. Oil Chem. Soc. 79 (2002) 797–802.
[40] L. Barral, J. Cano, A. López, P. Nogueira, C. Ramírez, Determination of the activation energies for α and β transitions of a system containing a diglycidyl ether of bisphenol a (DGEBA) and 1,3-bisaminomethylcyclohexane (1,3-BAC), J. Therm. Anal. Calorim. 41 (1994) 1463–1467.
[41] G. Li, P. Lee-Sullivan, R. Thring, Determination of activation energy for glass transition of an epoxy adhesive using dynamic mechanical analysis, J. Therm. Anal. Calorim. 60 (2000) 377–390.
[42] W.K. Goertzen, M.R. Kessler, Dynamic mechanical analysis of carbon/epoxy composites for structural pipeline repair, Compos. Part B Eng. 38 (2007) 1–9.
[43] L. Núñez, F. Fraga, A. Castro, L. Fraga, Elastic moduli and activation energies for an epoxy/m-XDA system by DMA and DSC, J. Therm. Anal. Calorim. 52 (1998) 1013–1022.
[44] S. Tatsumiya, K. Yokokawa, K. Miki, A dynamic DSC study of the curing process of epoxy resin, J. Therm. Anal. Calorim. 49 (1997) 123–129.
[45] H.W. Starkweather, Simple and complex relaxations, Macromolecules 14 (1981) 1277–1281.
[46] H.W. Starkweather, Noncooperative relaxations, Macromolecules 21 (1988) 1798–1802.
[47] L. Heux, F. Lauprêtre, J.L. Halary, L. Monnerie, Dynamic mechanical and 13C n.m.r. analyses of the effects of antiplasticization on the [beta] secondary relaxation of aryl-aliphatic epoxy resins, Polymer 39 (1998) 1269–1278.
[48] L. Heux, J.L. Halary, F. Lauprêtre, L. Monnerie, Dynamic mechanical and 13C n.m.r. investigations of molecular motions involved in the [beta] relaxation of epoxy networks based on DGEBA and aliphatic amines, Polymer 38 (1997) 1767–1778.
[49] J.M.J. Fréchet, D.A. Tomalia, Dendrimers and Other Dendritic Polymers, John Wiley & Sons, Ltd., 2001.